Kinematic Inversion of the 2004 M_w6 Parkfield Earthquake from Strong-Motion Data and High-Rate GPS Data

(1)University of California at Santa Barbara
(2)University of Colorado at Boulder

Susana Custódio[1] susana@crustal.ucsb.edu Ralph Archuleta[1] ralph@crustal.ucsb.edu Pengcheng Liu[1] pcliu@crustal.ucsb.edu Kristine Larson[2] Kristine.Larson@colorado.edu

FCT Fundação para a Ciência e a Tecnologia
MINISTÉRIO DA CIÊNCIA, TECNOLOGIA E ENSINO SUPERIOR Portugal

an NSF+USGS center

The 2004 M_w6 Parkfield Earthquake

Parkfield marks the transition between a seismically locked section (SE) and a creeping section (NW) of the San Andreas Fault (SAF). Bakun and McEvilly (1984) noticed that Parkfield experienced moderate - M_w6 - earthquakes in average every 22 years. They furthermore observed that the Parkfield earthquakes were identical in terms of epicenter, direction of rupture, ground-motion generated and foreshocks. Thus, Bakun and McEvilly (1984) proposed that Parkfield earthquakes were "characteristic", and predicted that the next Parkfield earthquake would occur between 1983 and 1993. Having evaluated and accepted this prediction, the USGS deployed a network of geophysical instruments to trap the next Parkfield earthquake. The 2004 Parkfield earthquake was therefore very well recorded by strong-motion seismographs and GPS 1-Hz receivers, among many other instruments. The high-quality dataset available for this earthquake allows us to investigation what is the best way to combine GPS and seismic data. In this poster, we present a two-step approach to combine the two types of data (seismic and GPS) that consists on: 1) Invert the GPS data; 2) Use the seismic moment and slip distribution inferred from GPS data to constrain the inversion of strong-motion data.

Figure 1. Map of California showing the different segments of the San Andreas Fault (SAF). The red sections slip in great earthquakes (M_w~8), with long recurrence intervals (~ hundreds of years). The gray section are marked by abundant microseismicity and surface creep. Parkfield is located between a region of creep and a locked part of the SAF.

1. Obtaining a rupture model – kinematic inversion

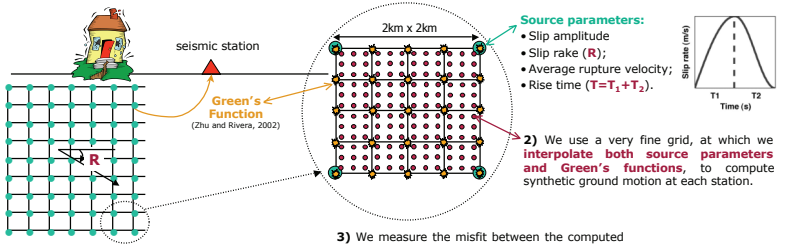

1) We assume that the ground motion at a given station can be described as a sum of the slip on discrete points of the fault convolved with their Green's function.

Some assumptions of our model:

- ✓ The fault strikes 140º SE and dips 87º SW;
- ✓ The rupture was at maximum 40 km long;
- ✓ The ruptured area is deeper than 0.5 km (no surface rupture);
- ✓ The velocity structure is well approximated by a 1D bilateral model (NE – slow; SW – fast; after Eberhart-Phillips and Michael (1993) and Thurber et al. (2003)).

2) We use a very fine grid, at which we **interpolate both source parameters and Green's functions**, to compute synthetic ground motion at each station.

3) We measure the misfit between the computed synthetics and observed data. We compute synthetics for many different sets of source parameters. The goal of our simulated annealing global inversion scheme is to obtain a rupture model that generates synthetics with the smallest misfit to data (Liu and Archuleta, 2004).

In order to make use of both the wave field and static field information contained in the GPS data, we compare the initial and final parts of the GPS 1-Hz records to the synthetics. For strong-motion data, we use only the initial part of the record. By not using the rest of the records, we diminish the weight of data noise in our inversions.

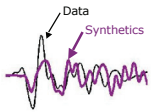

2. Slip model from inversion of GPS 1-Hz data

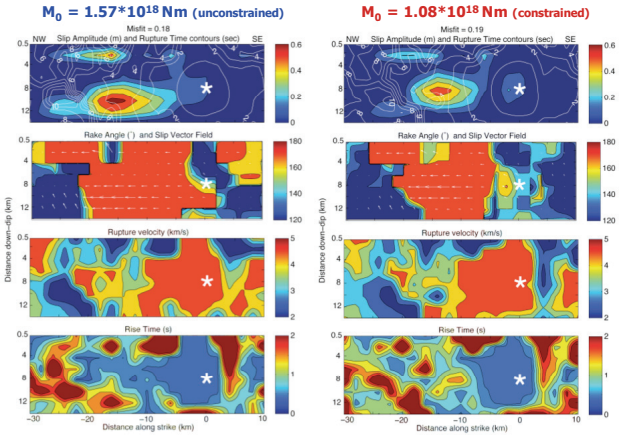

Figure 2. Space-time slip model for the 2004 Parkfield earthquake obtained from the inversion of 1-Hz GPS data. The left column shows the model obtained when the seismic moment M_0 is not constrained. The right column shows the rupture model obtained when M_0 is constrained. Both models are adequate, i.e., both rupture models generate waveforms that fit the observed data well (the misfits between observed and synthetic ground-motion is very similar for both models).

Both models show that slip occurred mainly at a depth between 6 and 12 km, NW of the hypocenter. Shallow slip NW of the hypocenter is also a feature of the two models

Figure 3. Fit between GPS-observed static offsets and synthetic static offsets generated by the two rupture models above. The gray dots are aftershocks (Thurber et al., in press); the red star marks the epicenter; the red line is the projection on the surface of the modeled fault plane. The synthetic static offsets fit the observed data well, both when the seismic moment is constrained, and when it is not constrained. The major difference between the two models is at stations POMM. The horizontal displacement at this station is much better fit by the unconstrained model. Because vertical records are more noisy, we downweighted them in our inversion. Therefore, vertical displacements are not as well fit as horizontal. Despite the strong downweighting of vertical observations, most of the vertical records are well fit by our models.

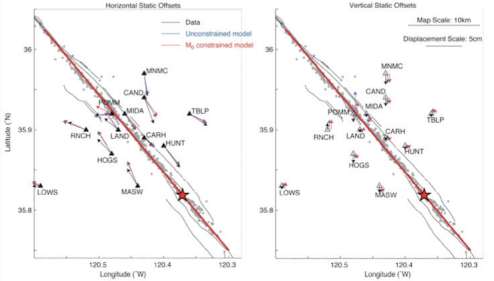

Figure 4. Fit between GPS-observed displacements (black) and synthetic ground-motion generated by our unconstrained rupture model (red).

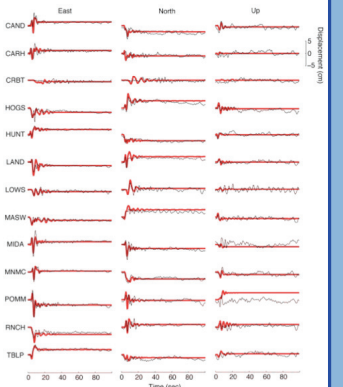

3. Seismic data constrained inversion

Figure 5. Inversion of strong-motion seismic data constrained by GPS data: 1) The seismic moment is constrained by the one derived from GPS observations; 2) The slip amplitude is constrained to be similar to the one obtained by inversion of GPS data.

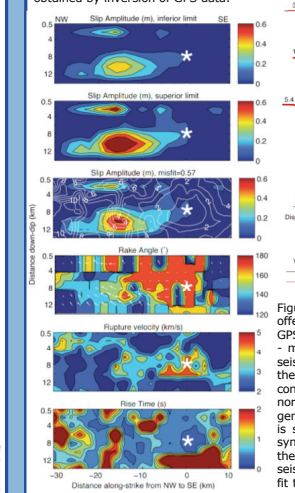

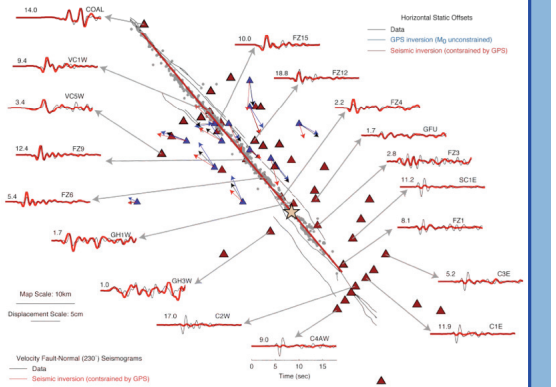

Figure 6. Map of the Parkfield section of the San Andreas Fault, showing the fit to data offered by the rupture model inferred from the inversion of seismic data constrained by GPS data. Small gray dots - aftershocks (Thurber et al., in press); star - epicenter; red line - modeled fault plane; blue triangles - 1-Hz GPS stations; red triangles - strong-motion seismic stations. Also shown are the static offsets observed with GPS (black), predicted by the model obtained by inversion of GPS data (blue) and by the model obtained by constrained inversion of seismic data (red). The seismograms are velocity records of fault-normal (230°) observed ground-motion (black) and synthetic ground-motion (red) generated by the constrained seismic inversion (figure 5). The maximum observed velocity is shown on the left-hand side of the seismogram in cm/s. We note that whereas the synthetic seismograms fit the observations quite well NW of the epicenter, toward the SE the ground-motion is strongly underpredicted. This is due to the GPS constrain on the seismic inversion, which does not allow slip to occur on the SE end of the fault plane. The fit to the static offsets offered by the constrained seismic model is adequate, despite being worse than the fit offered by the GPS-derived model.

Discussion and Conclusions

1) The GPS and seismic datasets complement each other: 1) the GPS dataset offers a constraint on seismic moment M_0, i.e., a constraint on the total amount of slip that occurred during the earthquake, that the seismic data cannot resolve; 2) Due to the geometry of the GPS network, GPS data cannot resolve slip toward the SE end of the fault plane that the seismic data can image. Care must be taken when using the two datasets together so that the information present in one dataset is not "erased" by the other dataset.

2) Care must be taken when using GPS data to constrain seismic moment. Our results indicate that it is possible to obtain considerably different seismic moment values due to only one station. In this work, we find two rupture models with different M_0 that generate very similar fits to all data except at one station (POMM). Thus, site effects that affect GPS data may have a big influence on the inferred seismic moment.

References
Bakun, W., and T. McEvilly (1984). Recurrence models and Parkfield, California, earthquakes, *Journal of Geophysical Research*.
Eberhart-Phillips, D and A. J. Michael (1993), Three-dimensional velocity structure, seismicity, and fault structure in the Parkfield Region, central California, *J. of Geophys. Res.*, 98.
Liu, P., and R. Archuleta (2004). A new nonlinear finite fault inversion with three-dimensional Green's functions: application to the 1989 Loma Prieta, California, earthquake, *Journal of Geophysical Research*.
Thurber, C., S. Roecker, K. Roberts, M. Gold, L. Powell, and K. Rittger (2003), Earthquake locations and three-dimensional fault zone structure along the creeping section of the San Andreas fault near Parkfield, CA: Preparing for SAFOD, *Geophysical Research Letters*.
Thurber, C., H. Zhang, F. Waldhauser, J. Hardebeck, A. Michael and D. Eberhart-Phillips (in press). Three-dimensional compressional wavespeed model, earthquake relocations and focal mechanisms for the Parkfield, California, region, *Bulletin of the Seismological Society of America*.

Acknowledgments
The data we use was collected, pre-processed and made available by the California Geological Survey (CGS) and the United States Geological Survey (USGS). A cluster sponsored by Hewlett-Packard at the California NanoSystems Institute (CNSI), UC Santa Barbara, was used for the computations.